LiGaTe2: A New Highly Nonlinear Chalcopyrite Optical Crystal for the Mid-IR

ARTICLE *in* CRYSTAL GROWTH & DESIGN · JUNE 2005

Impact Factor: 4.89 · DOI: 10.1021/cg050076c

CRYSTAL GROWTH & DESIGN
2005
VOL. 5, NO. 4
1325−1329

$LiGaTe_2$: A New Highly Nonlinear Chalcopyrite Optical Crystal for the Mid-IR

L. Isaenko,[†] P. Krinitsin,[†] V. Vedenyapin,[†] A. Yelisseyev,[†] A. Merkulov,[†] J.-J. Zondy,[‡] and V. Petrov*[,#]

Branch of Institute of Mineralogy and Petrography, SB RAS, 43 Russkaya Street, 630058 Novosibirsk, Russia, Institut National de Métrologie, Conservatoire National des Arts et Métiers, 292 rue Saint-Martin, F-75003, Paris, France, and Max-Born-Institute for Nonlinear Optics and Ultrafast Spectroscopy, 2A Max-Born-Strasse, D-12489 Berlin, Germany

Received March 1, 2005; Revised Manuscript Received May 20, 2005

ABSTRACT: The chalcopyrite crystal $LiGaTe_2$ was grown by the Bridgman-Stockbarger technique with sufficient size and optical quality that allowed the characterization of its linear (dispersion and birefringence) and nonlinear optical properties. X-ray structural analysis was performed on single crystals. The transmission was recorded in the 0.5−24 μm range, and Raman and IR-spectra were recorded in the 0−400 cm^{-1} and 180−400 cm^{-1} ranges, respectively. The clear transparency range of $LiGaTe_2$ extends from 2.5 to 12 μm, the band-gap at room temperature is at 2.41 eV (515 nm), residual absorption limits the transmission near the band-edge, and the upper limit for the transmission is determined by the onset two-phonon absorption. $LiGaTe_2$ is a positive uniaxial crystal that possesses sufficient birefringence for phase-matching. Its nonlinear coefficient d_{36} was estimated by phase-matched second harmonic generation to be 43 pm/V ± 10%. It is only the third crystal belonging to the $A^IB^{III}C_2^{VI}$ chalcopyrite family for which phase-matched nonlinear frequency conversion could be demonstrated, and of this group it exhibits the highest nonlinearity and figure of merit for nonlinear optical applications in the mid-infrared.

The compound $LiGaTe_2$ (LGT) was mentioned for the first time in relation to possible tetragonal structures of the chalcopyrite type in the family of the $Li^IB^{III}C_2^{VI}$ chalcogenides,[1] where B^{III} = Al, Ga, In, and C^{VI} = S, Se, Te. On the basis of the so-called electronegativity differences, the authors who determined the space group ($I\bar{4}2d$ or D_{2d}^{12}, No. 122) of $LiInTe_2$ (LIT) predicted the same chalcopyrite ($CuFeS_2$) structure for LGT.[1] The existence of LGT was also predicted in a more general systematic survey of the $A^IB^{III}C_2^{VI}$-type compounds where A^I is an alkali metal and B^{III} = Ga, In, Tl.[2] On the basis of the dependence on the sum of the atomic numbers of the components, a melting temperature of 1002 K and a band-gap of 1.7 eV were predicted for LGT.[2]

The first LGT crystals, grown by the Tammann-Stöber technique,[3] were black and did not exhibit a single phase, decomposing within hours into small-grained mixtures of LGT, GaTe, and Te. Nevertheless, from powder X-ray diffraction it was possible to confirm the chalcopyrite structure of LGT and measure its lattice constants.[3] The melting temperature reported was 913 ± 10 K. It was only recently that the Bridgman-Stockbarger technique was successfully applied for the growth of LGT. This allowed us to confirm its noncentrosymmetric, chalcopyrite structure by powder X-ray diffraction and speculate on its potential as a nonlinear optical crystal.[4] Initial estimations of the crystal lattice parameters, the transparency range, and the band-gap were also presented in ref 4, but they were based on low-quality and relatively small LGT samples. Here we report on the improved growth of LGT with sizes that allowed us to record the transmission and Raman spectra, to evaluate the linear (dispersion, birefringence) and nonlinear optical properties, and to demonstrate phase-matched second harmonic generation (SHG).

The Bridgman-Stockbarger technique was used for the growth of LGT. The crystals were grown in a vertical two-zone furnace with a diaphragm. The temperature at which crystallization started was only several degrees lower than the melting temperature of the starting charge. The initial polycrystalline charge was obtained in a glassy carbon container. The elementary starting chemicals used for the synthesis had a purity of 99.99% (Li) and 99.999 (Ga and Te). The components were weighed with an accuracy of about 4 mg out of a total charge of 50 g. The composition of the starting charge differed from the stoichiometric one to account for the incongruent evaporation near the melting temperature connected with Li and Te loss[5] and the high chemical reactivity of Li-containing components and their interaction with the container walls.[6] Hence, the initial charge was rich in Li and Te. After the starting components were loaded into the ampule, it was evacuated to a residual pressure of 10^{-3} Torr and inserted into the vertical two-zone furnace where the components were alloyed for 4 h. The polycrystalline charge obtained was loaded in a dry chamber into a silica ampule with several layers of pyrolitic graphite deposited on its inner surface. To prevent dissociation of the compound, the free volume of the ampule was filled with purified Ar. The Ar pressure was selected to provide 1 atm at the growth temperature.

The sealed ampule was inserted then into the two-zone furnace for directed crystallization. To control the isotherm shape, a forced heat sink from the lower part of the ampule was arranged; for this purpose, a copper rod was placed inside the ampule. The ampule was heated slowly (for 16 h) until the whole content was melted at 940 ± 5 K, and only a seed crystal in its initial position remained solid. Then the temperatures in both zones of the furnace were held fixed for 1 day. Afterward, the mechanism for ampule shifting with a rate of 2−5 mm/day to the cold zone was switched on: typical values of the axial temperature gradient were about 2−4 °C/mm.

We established that the deviation from the stoichiometry in the melt is an important parameter that determines to a great extent the quality of the resulting crystals. Lithium deficit facilitates the crystallization of $LiGa_3Te_5$, which precludes the growth of large crystals of LGT. The presence of the $LiGa_3Te_5$ phase[7] in the boules grown with a Li deficit

* Corresponding author. Phone: ++49-30-6392 1272. Fax: ++49-30-6392 1289. E-mail: petrov@mbi-berlin.de.
[†] Branch of Institute of Mineralogy and Petrography.
[‡] Institut National de Métrologie.
[#] Max-Born-Institute for Nonlinear Optics and Ultrafast Spectroscopy.

10.1021/cg050076c CCC: $30.25
Published on Web 06/18/2005

Table 1. Atomic Coordinates and Isotropic Thermal Parameters U_{iso}

atom	x	y	z	U_{iso} [Å^2]
Li	0	0	0	0.026(9)
Ga	0.5	0	0.25	0.014(1)
Te	0.2666(1)	0.75	0.125	0.016(1)

was confirmed using powder X-ray structural analysis. Using the procedure described above, we were able to obtain for the first time single crystals of LGT with sufficient size (about 0.5 cm^3), which permitted us to study important physical properties.

Single-crystal X-ray structural analysis was performed at room temperature using a Bruker P4 diffractometer and the Mo Kα line ($\lambda = 0.71069$ Å), $2\theta_{max} = 60°$, $R_{int} = 0.047$. The updated lattice parameters are $a = 6.3295(6)$ Å, $c = 11.682(1)$ Å, $V = 468.0(1)$ Å^3, and $Z = 4$. The refinement was performed using the SHELXL97 program in an anisotropic approximation (Table 1).[8] The final residuals were R1 = 0.0272, wR2 = 0.0661 for 190 $F \geq 4\sigma(F)$, R1 = 0.0288, and wR2 = 0.0670 for all 208 unique reflections. The revised lattice constants measured with single crystals are smaller in comparison to ref 3 and our initial estimations,[4] where in both cases powder X-ray analysis was used. Note that from our experience with the related $LiInS_2$ higher quality crystals have smaller lattice constants.[6] Atomic coordinates and isotropic thermal parameters U_{iso} for LGT are given in Table 1.

The axial ratio $c/a \approx 1.85$ for LGT is less than 1.95, which means according to the empirical rules established for such ternaries[9] LGT will remain in the ordered chalcopyrite structure even at high temperatures. The axial ratio of a chalcopyrite is a measure of the uniaxial tetragonal distortion from the underlying diamond-like face-centered cubic structure. This distortion is relatively large in LGT (7.7%, see $c/2a$ values in Table 2), which means that substantial birefringence can be expected. For comparison, this distortion is comparable in $AgGaSe_2$ and maximum for $AgGaS_2$ (10.5%) (see Table 2).

The as-grown or cleaved LGT crystals have natural faces of complex shape and a different color depending on the thickness: from yellow for thin pieces to red and even black for thicker ones. LGT transmits up to 16 μm, but the clear transparency region extends from 2.5 to 12 μm (Figure 1). Residual absorption is present at shorter wavelengths. An intense absorption band centered near 16 μm with a shoulder near 19 μm can be observed in the transmission spectrum of LGT and more clearly in the absorption coefficient (Figure 1). This band serves as an upper limit for practical optical applications.

We recorded Raman spectra using a Bruker RFS 100/S spectrometer with 1064 nm (Nd:YAG laser) pumping in 180° geometry (Figure 2). The fragment of the IR absorption spectrum (180−400 cm^{-1}) was measured using a Bomem FTIR spectrometer. For a chalcopyrite $A^IB^{III}C_2^{VI}$-type structure with the space group $I\bar{4}2d$ symmetry allows vibration to be classified into 15 normal modes:[10] $\Gamma_O = A_1 + 2A_2 + 3B_1 + 3B_2 + 6E$, where B_2 and E are polar Raman active modes having transverse optical (TO) and longitudinal optical (LO) modes, A_1 and B_1 are nonpolar Raman active modes, and A_2 is an optically inactive mode. The Raman scattering intensity of the A_1 vibrational mode is much stronger than that of any other mode; this mode is associated with the vibrations of two pairs of anions. Its frequency is equal to $2(f_A + f_B)/m_C$ where f terms are the corresponding force constants and m is the atomic mass.[11] The B_2 and E vibrational modes are IR active and associated with anions and cations.[10,11]

Four groups of peaks can be seen in the Raman spectra (Figure 2). The dominating A_1 peak at 120.4 cm^{-1}, related to Te vibrations, exhibits a shoulder at 141.6 cm^{-1}. The same A_1 mode is at 122 cm^{-1} in LIT.[3] Its frequency is inversely proportional to the square root of the anion atomic weight[11] and according to ref 10 also inversely proportional to the square root of the cation mean atomic weight. The first dependence seems to be fulfilled if we compare it with $LiGaS_2$ and $LiGaSe_2$.[12] Although these related lithium compounds have β-$NaFeO_2$ (wurtzite-type) structure, a similar dominating line with A_1 symmetry is observed in them, too.[3] The second dependence can be checked by comparison with the A_1 modes of LIT[3] and $AgGaTe_2$.[10] It is not fulfilled, which can be attributed to the different binding nature of the Li-containing chalcopyrites in which the Li atoms are rather weakly bound to the Te atoms.[13]

The low-frequency vibrations are characterized by a peak at 49.1 cm^{-1} with a shoulder at 39.4 cm^{-1} and a stronger line at 76.1 cm^{-1} (similar to the one observed in LIT[3]) with weaker 87.5 and 97.2 cm^{-1} peaks seen as shoulders in Figure 2. Two groups of lines are observed at higher frequencies whose relative intensity depends on the crystal orientation (Figure 2). The first group near 200 cm^{-1} consists of peaks at 195.6, 197.5, 211.0, and 220.7 cm^{-1}. In the second group two peaks at 303.6 and 324.8 cm^{-1} are dominating, whereas additional ones at 320.9, 295.8, 309.4, and 340.3 cm^{-1} are observed as shoulders. Similar groups of peaks at higher frequencies can be found in the IR absorption spectra in Figure 2. The second group near 300 cm^{-1} can be ascribed to sphalerite-like Li−Te vibrations (E^3 and B_2^2 modes[11]), as in LIT where very close modes at 302.7 cm^{-1} (TO) and 315.3 cm^{-1} (LO) were derived from IR reflectance spectra.[13] The group of lines near 200 cm^{-1} is related to sphalerite-like Ga−Te vibrations.[11] The same modes in LIT are shifted to 168.2 cm^{-1} (TO) and 180.8 cm^{-1} (LO) in reflectance measurements[13] or close to 180 cm^{-1} from Raman spectra,[3] as can be expected for the heavier In atoms. They are in the range 198−220.7 cm^{-1} in $AgGaTe_2$ (ref 14), which is clear from the fact that the E^1 and B_2^1 modes should have equal frequencies in compounds with the same B^{III} and C^{VI} elements.[11] The force constants of the Li^I−Te^{VI} and Ga^{III}−Te^{VI} bonds can be estimated using the valence-force-field model of Keating[11] from $\omega^2(Li-Te,Ga-Te) = 4f_{Li,Ga}[m_{Li,Ga}^{-1} + m_{Te}^{-1}]$. Taking the values of 200 and 300 cm^{-1} as average frequencies of the above-mentioned sphalerite-like modes we obtained $f_{Li} = 8.7$ N/m and $f_{Ga} = 26.4$ N/m. These values are similar to those for LIT (8.9 and 25.1 N/m, respectively).[13] One can see that f_{Li} (LGT) is considerably smaller than $f_{Ag}(AgGaTe_2) = 22.7$ N/m,[11] which clearly indicates that, as in LIT,[13] the Li atoms in LGT are rather weakly bound to the Te atoms. Hence it is justified to conclude, as for LIT,[11] that the Li atoms should have a high mobility in the LGT lattice and the Li−Te bond is essentially ionic in nature.[2]

The high-frequency limits near 360 cm^{-1} for the vibrational IR absorption/Raman spectra of LGT in Figure 2 correlate with the transmission limit of 13.8 μm (Table 2), which can be associated with two-phonon absorption. Similarly, the maximum of the absorption near 16 μm in Figure 1 correlates with the two-phonon energy of the vibrational modes centered near 300 cm^{-1} in Figure 2, and the onset of further absorption above 22 μm and the actual mid-IR transparency edge are related to two-phonon absorption involving the next vibrational band near 200 cm^{-1}.

The transmission limits of LGT at an absorption level of 3 cm^{-1} are included in Table 2 for comparison with other chalcopyrites: at a level of 5 cm^{-1} they are close to our previous estimations,[4] and at a level of 10 cm^{-1} they extend

Table 2. Chalcopyrite Crystals of the $A^{I}B^{III}C_2^{VI}$-Type for the Nonlinear Optics[a]

	E_g [eV]	n (5.3 μm)	$c/2a$	$n_e - n_o$ (5.3 μm)	d_{36} [pm/V] 5.3 → 2.65μm	T [μm]	d_{36}^2/n^3 [pm^2/V^2]
$AgGaS_2$	2.75	2.37	0.895	−0.054	12.7	0.5−13.2	12
$AgInS_2$	2.03	2.40[b]	0.960	−0.012[b]	15	0.72−14.3	16
$AgGaSe_2$	1.83	2.60	0.908	−0.033	35	0.78−18	70
$AgInSe_2$	1.24	2.64	0.957	0.003	39.7	1.1−21	85
$AgGaTe_2$	1.32	2.98	0.953	0.016	76.6[c]	1.4−21	222[c]
$AgInTe_2$	1.03	3.03[d]	0.981		84.7[c]		258[c]
$LiGaTe_2$	2.41	2.54	0.923	0.094	42	0.95−13.8	105
$LiInTe_2$	1.5	2.81[d]	0.974		59[c]		156[c]

[a] E_g: direct band-gap, n: average refractive index, $c/2a$: tetragonal distortion, d_{36}: nonlinear coefficient, T: transparency at a level of 3 cm^{-1}, d_{36}^2/n^3: figure of merit. [b] Extrapolation from $AgGa_{1-x}In_xS_2$ (x = 0.2, 0.6) data. [c] Theoretical estimations based on relative band-gap values. [d] From static dielectric constant.

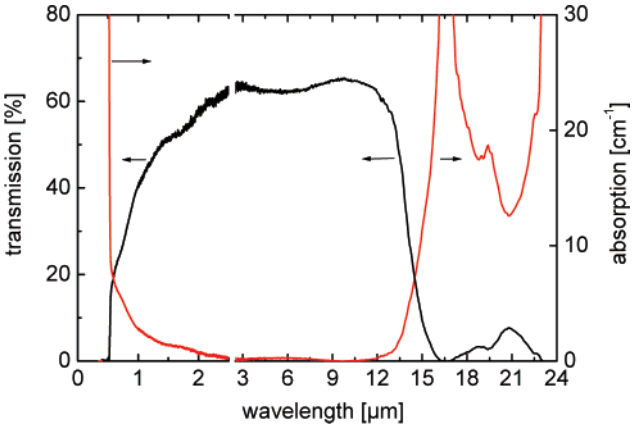

Figure 1. Unpolarized transmission recorded for a 1.7-mm-thick yellow LGT sample and the corresponding absorption coefficient.

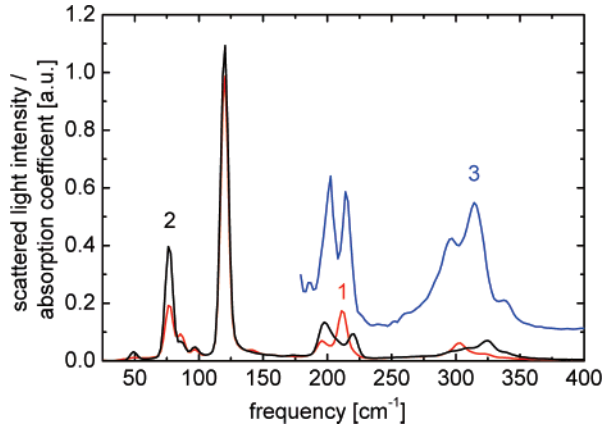

Figure 2. Raman (1 and 2) and IR absorption (3) spectra, recorded for a polished (001) plate (1), a cleaved plate with natural (unpolished) faces of arbitrary orientation (2), and powder mixture of LGT/CsI (3). The IR spectrum (3) is shifted upward for clarity. Cesium iodate (CsI) powder is used to dilute the LGT powder in the region of strong absorption.

from 0.54 to 14.85 μm. For the band-gap measurements a thin (≈250 μm) yellow plate of LGT with natural faces was used. The fundamental absorption edge was measured at 11 different temperatures from 80 to 325 K. The recorded curves can be approximated with straight lines in the coordinates α^2 and $h\nu$, where α is the absorption coefficient in cm^{-1} and $h\nu$ is the photon energy in eV. The straight-line approximation is applied to the rapidly increasing portions of the curves in Figure 3. Thus, the fundamental absorption edge is described by the $\alpha = A(h\nu - E_g)^{1/2}$ dependence, where A is a constant and the band-gap E_g can be determined from the cross points of the straight lines with the abscissa. This dependence corresponds to direct allowed electronic transitions.[15] In the inset of Figure 3 the band-gap values are plotted versus temperature T. The band-gap is 2.65 and 2.41 eV at 80 and 300 K, respectively. It depends linearly on temperature and $dE_g/dT = -1.106 \times 10^{-3}$ eV/K. The band-gap of LGT is substantially larger than the predictions of ref 2 (1.7 eV). It is interesting to note that E_g(LGT) substantially exceeds also the band-gap value known for the isostructural $AgGaTe_2$ (1.316 eV).[16]

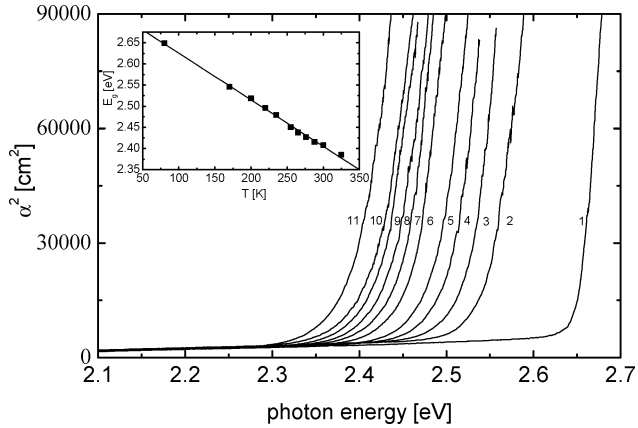

Figure 3. Absorption coefficient near the band edge of LGT measured at temperatures 80, 170, 200, 220, 235, 255, 265, 276, 288, 300, and 325 K (curves 1−11, respectively) plotted in coordinates α^2 and $h\nu$. The inset shows the temperature dependence of E_g (LGT) obtained (squares) and its linear fit (line).

The variation of the LGT color from yellow to black (opaque for visible light) is a result of composition deviation from stoichiometry and the presence of native point defects in the bulk or the near surface layer in the case of polishing. The smooth transparency variation at shorter wavelength is indicative of light scattering or inclusions of side phases. As in the case of other multicomponent chalcogenides, an additional high-temperature annealing in special atmosphere is expected to improve the transparency in this spectral region.

The LGT refractive indices for the two polarizations were measured at room temperature by the minimum deviation technique using a semiprism for 10 wavelengths from 0.8 to 10 μm (Figure 4). The beam from an incandescent lamp or from a globar, after wavelength selection by a prism monochromator, was directed to the LGT semiprism positioned on the axis of a goniometer. A cooled photomultiplier, a Ge phototransistor, or a cooled HgCdTe detector was used for detection. The beam-shaping optics contained only reflective elements (systems of cylindrical concave mirrors) to minimize the wavelength dependence. The desired polarization was selected using a set of film or grid polarizers. The experimental points, obtained for the ordinary and extraordinary beams, are included in the table in Figure 4. One can see that n_e is larger than n_o; hence, LGT is a positive uniaxial crystal like $ZnGeP_2$ (ZGP)

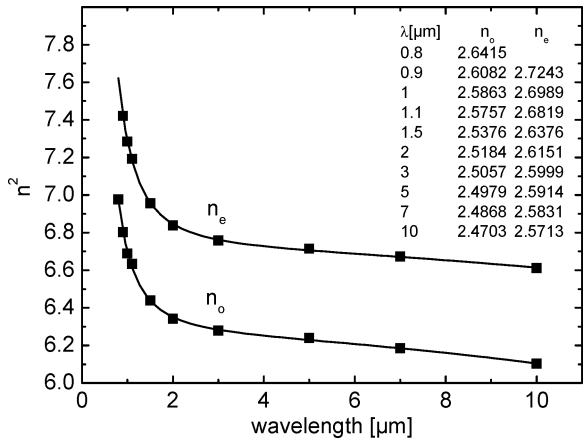

Figure 4. Squared refractive index of LGT: experimental points (squares) and Sellmeier fits (lines). The table gives the measured values of the ordinary and extraordinary refractive indices.

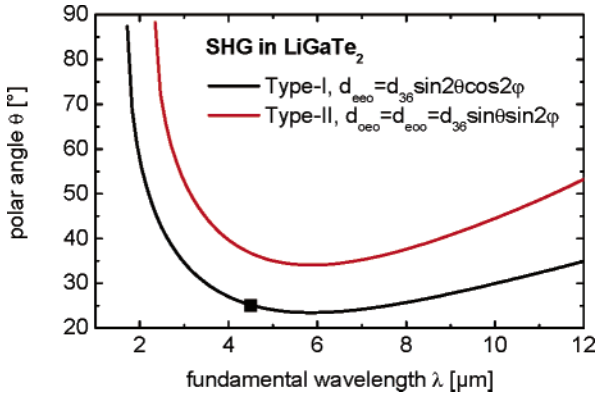

Figure 5. Calculated SHG phase-matching in LGT (curves) and experimental point (square) at $\lambda = 4.5$ μm.

and $AgGaTe_2$, all three of them having the same point group $\bar{4}2m$. In contrast to $AgGaTe_2$,[16,17] however, the birefringence of LGT ($n_e - n_o \approx 0.1$) is sufficient for phase-matching. The refractive indices of LGT were fitted to single-pole Sellmeier equations containing an IR-term, $n^2 = A + B/(\lambda^2 - C) - D\lambda^2$, where $A_o = 6.24921$, $B_o = 0.42592$, $C_o = 0.0531$, $D_o = 0.00149$, $A_e = 6.70825$, $B_e = 0.5667$, $C_e = 0.01964$, $D_e = 0.001$, and the wavelength λ is measured in micrometers. The fits are also plotted in Figure 4 together with the experimental points.

The calculated phase-matching angles for SHG and the expressions for the corresponding effective nonlinearities are shown in Figure 5. We estimated the nonlinear coefficient d_{36} of LGT by comparing the SHG (type-I) conversion efficiency at 4.5 μm to that obtained with ZGP, using 250-fs pulses of 2 μJ energy generated by a $KNbO_3$ parametric amplifier operating at 1 kHz. Both samples were uncoated and 2-mm thick. The LGT sample was cut at $\theta = 25°$, $\varphi = 27°$. The ZGP sample was cut at $\theta = 52.5°$, $\varphi = 0°$. It was grown at Sanders and exhibited negligible residual absorption at the second harmonic at 2.25 μm.[18] Taking into account the different refractive indices, Fresnel reflections, absorption losses of LGT at the fundamental and second harmonic, and d_{36}(ZGP) = 75 pm/V,[18] we arrived at d_{36}(LGT) = 43 pm/V ± 10%. The experimental angle was in excellent agreement (<0.2°) with the calculated one. Thus, LGT is a highly nonlinear optical crystal whose nonlinear coefficient is about 7 times that of the related orthorhombic $LiGaS_2$[19] and about 4.5 times that of $LiGaSe_2$.[19]

A summary of the relevant linear and nonlinear optical properties of those chalcopyrite compounds belonging to the $A^IB^{III}C_2^{VI}$ family that are interesting for nonlinear optics is given in Table 2. For comparison all the data available are reduced (whenever possible) to 5.3 μm using Miller's rule for the nonlinear polarizability. Some of the data in Table 2 is based on theoretical estimations. For the estimation of d_{36}(LIT), we used the ratio of the band-gap values (1.5:1.7) relative to LGT.[2] Note that only gallium compounds exhibit sufficient birefringence, and only two of these crystals ($AgGaS_2$ and $AgGaSe_2$) are widely used and are commercially available. The indium compounds in general have too low birefringence. $AgInS_2$ and $AgInSe_2$ have been used in the past only for engineering of solid solutions of the types $AgGa_{1-x}In_xS(e)_2$ by reducing the birefringence of the corresponding gallium compounds. From the values of the tetragonal distortion parameter $c/2a$, it can be expected that $AgInTe_2$ and LIT, for which no data on the refractive indices exist, also do not possess sufficient birefringence. Note that the birefringence of $AgGaTe_2$ is slightly too low for phase-matching, and it was only suggested that solid solutions of the type $AgGa(Se_{1-x}Te_x)_2$, with nonlinearity exceeding that of $AgGaSe_2$, might be useful.[16] Thus, the compound LGT is the third chalcopyrite of the $A^IB^{III}C_2^{VI}$ type for which a phase-matched nonlinear optical process has been demonstrated. At the same time, it should be outlined that LGT exhibits the largest birefringence and highest nonlinearity and figure of merit (d_{36}^2/n^3) as compared to $AgGaS_2$ and $AgGaSe_2$ (Table 2).

In conclusion, we demonstrated that the newly synthesized ternary semiconductor LGT belonging to the chalcopyrite class is a promising material for nonlinear optical applications in the mid-IR. In particular, LGT is transparent and phase-matchable for frequency doubling of CO_2 laser radiation at 10.6 μm. Future studies will be devoted to the thermomechanical and thermooptical properties of LGT, improvement of the crystal transmission, and polishing techniques.

Acknowledgment. This work was supported by the Russian Foundation for Basic research (Grant 04-02-16334) and the BMBF program (Russia-Germany) WTZ (Grant RUS 01/223). We thank Dr. P. Schunemann (Sanders, now BAE Systems Company) for the high-quality ZGP sample used in the present work and an anonymous reviewer who helped us to improve the readability of the manuscript.

References

(1) Hönle, W.; Kühn, G.; Neumann, H. *Z. Anorg. Allg. Chem.* **1986**, *532*, 150.
(2) Kish, Z. Z.; Peresh, E. Yu.; Lazarev, V. B.; Semrad, E. E. *Inorg. Mater.* (*Engl. Transl.*) **1987**, *23*, 697; *Izv. Akad. Nauk SSR, Neorg. Mater.* **1987**, *23*, 777.
(3) Brückner, J. I−III−VI−Verbindungshalbleiter mit Lithium als Gruppe I-Element: Kristallzüchtung und Charakterisierung, Dissertation, Albert-Ludwigs-Universität, Freiburg i. Br., Germany, 1997.
(4) Isaenko, L.; Yelisseyev, A.; Lobanov, S.; Titov, A.; Petrov, V.; Zondy, J.-J.; Krinitsin, P.; Merkulov, A.; Vedenyapin, V.; Smirnova, J. *Cryst. Res. Technol.* **2003**, *38*, 379.
(5) Isaenko, L.; Vasilyeva, I.; Merkulov, A.; Yelisseyev, A.; Lobanov, S. *J. Cryst. Growth* **2005**, *275*, 217.
(6) Isaenko, L.; Vasilyeva, I.; Yelisseyev, A.; Lobanov, S.; Malakhov, V.; Dovlidova, L.; Zondy, J.-J.; Kavun, I. *J. Cryst. Growth* **2000**, *218*, 313.
(7) Kienle, L.; Deiseroth, H.-J. *Z. Kristallogr.* **1998**, *213*, 20.
(8) Naumov, D. Y.; Boldyreva, E. V. *J. Struct. Chem. (Engl. Transl.)* **1999**, *40*, 86; *Zh. Strukt. Khim.* **1999**, *40*, 102.
(9) Binsma, J. J. M.; Giling, J. L.; Bloem, J. *J. Cryst. Growth* **1980**, *50*, 429.
(10) Matsushita, H.; Endo, S.; Irie, T. *Jpn. J. Appl. Phys.* **1992**, *31*, 18.
(11) Neumann, H. *Helv. Phys. Acta* **1985**, *58*, 337.

(12) Eifler, A.; Riede, V.; Brückner, J.; Weise, S.; Krämer, V.; Lippold, G.; Schmitz, W.; Bente, K.; Grill, W. *Jpn. J. Appl. Phys.* **2000**, *39* (Suppl. 39-1), 279.
(13) Kühn, G.; Schumann, B.; Oppermann, D.; Neumann, H.; Sobotta, H. *Z. Anorg. Allg. Chem.* **1985**, *531*, 61.
(14) Kanellis, G.; Kampas, K. *J. Physique* **1977**, *38*, 833.
(15) Pankove, J. I. Optical Processes in Semiconductors; Prentice-Hall: Englewood Cliffs, NJ, 1971; p 456.
(16) Ohmer, M. C.; Goldstein, J. T.; Zelmon, D. E.; Saxler, A. W.; Hedge, S. M.; Wolf, J. D.; Schunemann, P. G.; Pollak, T. M. *J. Appl. Phys.* **1999**, *86*, 94.
(17) Shunemann, P. G.; Setzler, S. D.; Pollak, T. M.; Ohmer, M. C.; Goldstein, J. T.; Zelmon, D. E. *J. Cryst. Growth* **2000**, *211*, 242.
(18) Petrov, V.; Rotermund, F.; Noack, F.; Schunemann, P. *Opt. Lett.* **1999**, *24*, 414.
(19) Petrov, V.; Yelisseyev, A.; Isaenko, L.; Lobanov, S.; Titov, A.; Zondy, J.-J. *Appl. Phys. B* **2004**, *78*, 543.

CG050076C